phys. stat. sol. (b) **245**, No. 10, 2243–2246 (2008) / **DOI** 10.1002/pssb.200879598

physica status solidi b
www.pss-b.com
basic solid state physics

Exciton transfer and propagation in carbon nanotubes studied by near-field optical microscopy

Huihong Qian[1], Carsten Georgi[1], Neil Anderson[2], Alexander A. Green[3], Mark C. Hersam[3], Lukas Novotny[2], and Achim Hartschuh[1,*]

[1] Department Chemie und Biochemie and CeNS, Ludwig-Maximilians-Universität München, 81377 München, Germany
[2] University of Rochester, The Institute of Optics, Rochester, New York 14627, USA
[3] Department of Materials Science and Engineering, Department of Chemistry, Northwestern University, Evanston, Illinois 60208-3108, USA

Received 30 April 2008, revised 1 July 2008, accepted 1 July 2008
Published online 8 September 2008

PACS 68.37.Uv, 71.35.-y, 78.55.Ap, 78.67.Ch

* Corresponding author: e-mail achim.hartschuh@cup.uni-muenchen.de, Phone: ++49 (89) 2180-77515, Fax: ++49 (89) 2180-77188

We studied transfer and propagation of excitons in single semiconducting carbon nanotubes using high resolution tip-enhanced near-field photoluminescence microscopy. Exciton energy transfer is found to occur from a larger band gap nanotube to a smaller band gap nanotube. Efficient transfer however is found to be limited to a few nanometers because of competing fast non-radiative relaxation and can be explained in terms of electromagnetic near-field coupling. Towards the end of a nanotube, photoluminescence decay is observed on a length scale of 50-90 nm which is attributed to exciton propagation followed by additional non-radiative relaxation at the nanotube end.

1 Introduction The observation of photoluminescence (PL) from individual semiconducting single-walled carbon nanotubes (SWNTs) [1] underlined their enormous potential for photonic and optoelectronic applications and initiated a novel field of research. PL of semiconducting nanotubes arises from excitons with Bohr-radii of 2-5 nm that decay on picosecond time-scales [2–6]. Observation of PL energies and dynamics from single nanotubes provides access to the properties of excitonic states in SWNTs with specific chirality (n,m) [7–9]. Compared to diffraction limited conventional confocal microscopy, near-field microscopy offers high spatial resolution optical information resolving relevant length scales, such as the exciton diffusional range [10, 11].

In this work we use tip-enhanced near-field optical microscopy (TENOM) [12–14] as a tool to visualize and characterize PL along nanotubes. Near-field PL and topography images of a single nanotube bundle reveal the presence of two semiconducting nanotubes with different chiralities having an inter-nanotube spacing ranging from 1.5 to 4 nm. Anti-correlated intensity variations of the PL along the nanotubes are assigned to distance dependent exciton energy transfer. From the experimental data, we estimate transfer efficiencies. Towards the end of a nanotube, PL decay is observed on a length scale of 50-90 nm.

2 Experimental Our near-field optical setup is based on an inverted confocal microscope with an x, y scan stage for raster scanning a transparent sample [12–14]. A sharp gold tip is positioned in the focus of the laser beam and maintained above the sample surface at a distance of ≈ 2 nm by means of a sensitive shear-force feedback mechanism [15]. A near-field optical image is established by raster scanning the sample and simultaneously recording topographic and optical signals. CoMoCAT SWNTs were sorted by using discriminating surfactants and wrapped by DNA after sorting. The density gradient ultracentrifugation isolates the narrow distributed, chirality enriched nanotubes [16–18]. The sample studied in this paper was made by spin-coating the nanotube solution on a freshly cleaved

thin layer of mica glued on a glass cover slide. The mica layer was positively charged with Mg^{2+} ions by exposure to 1 M $MgCl_2$ to make the negatively charged DNA-site of the hybrid adhered to the surface [19].

3 Near-field PL spectroscopy of SWNTs: Imaging of mobile excitons

3.1 Resonant energy transfer in a pair of SWNTs

It is generally expected that bundling leads to quenching of the PL from nanotubes with large bandgap caused by rapid energy transfer to small bandgap and metallic nanotubes [1, 20–23]. Up to now, the range of energy transfer and its efficiencies were unknown. In ensemble measurements, the identification of donor and acceptor spectral signatures is complicated by overlapping contributions from different nanotube species, including phonon-assisted absorption and possible emission from lower lying defect-associated states. In the following, we present near-field optical imaging on chirality-assigned nanotubes forming a thin bundle.

Figure 1 presents PL images of DNA-wrapped nanotubes on mica. Figure 1(a) represents the intensity detected by an avalanche photodiode (APD) in the spectral range from 860-1050 nm, whereas Figs. 1(b),(c) are derived from spectra taken at each pixel. After splitting the emission into selected spectral windows, the structure extending from the upper left to the lower right is found to contain two clearly distinct emission peaks originating from a $(9,1)$ and a $(6,5)$ nanotube as evidenced by the emission energies of about 925 nm and 1000 nm (inserted spectra in Figs. 1(b) and (c)). The red-shift compared to the 912 nm emission energy reported for the $(9,1)$ nanotube and the 975 nm for $(6,5)$ [24] results from DNA-wrapping [25].

Emission from the $(9,1)$ nanotube (Fig. 1(b)) occurs in four bright segments, while emission from the $(6,5)$ nanotube (Fig. 1(c)) is more extended for about 1 µm. As four independent short $(9,1)$ nanotubes attached regularly along the $(6,5)$ nanotube would be very unlikely and since the PL of the $(9,1)$ does not disappear completely in between the bright segments, it is evident that we observe a bundle formed by a $(9,1)$ and a $(6,5)$ nanotube.

Remarkably, the PL of the $(6,5)$ nanotube is found to be stronger when the PL of the $(9,1)$ nanotube decreases (dashed arrow 1 in Figs. 1(b,c)). Strong PL of the $(9,1)$ nanotube on the other hand occurs in sections where $(6,5)$ emission is weaker (dashed arrow 2 in Figs. 1(b,c)). We attribute this anti-correlation of the PL intensities to energy transfer from the large bandgap $(9,1)$ nanotube to the small bandgap $(6,5)$ nanotube as expected for bundles. However, the fact that PL from $(9,1)$ is still detectable even within the bundle clearly shows that the efficiency of the energy transfer is limited. Spatial variations of the transfer efficiency can be understood in terms of varying inter-nanotube distance. The finite length of DNA-segments and the resulting partial DNA-wrapping could allow for different nanotube-nanotube spacing.

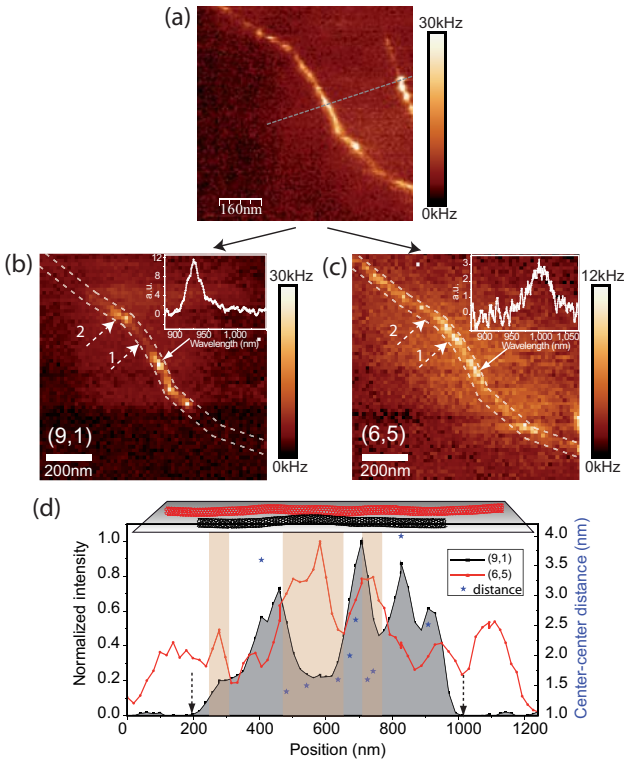

Figure 1 Near-field PL image (a) in the spectral range from 860 nm to 1050 nm. (b) and (c) represent the integrated intensities within selected spectral windows ranging from 910 to 940 nm for (b) covering the emission of $(9,1)$ nanotubes and from 990 to 1020 nm for (c) covering the $(6,5)$ emission. Evidently, the nanotube structure is a nanotube bundle composed of two nanotubes with different chiralities. The chirality assignment is based on the emission spectra detected at the positions marked with the white arrows shown in (b) and (c) that exhibit the characteristic energies of $(9,1)$ and $(6,5)$ nanotubes, respectively. Laser excitation at 632.8 nm with 100 µW and an integration time of 400 ms per spectrum were used. (d) presents intensity profiles taken along the $(9,1)$ (black line) and the $(6,5)$ nanotube (red line) summed between the two dashed lines in (b) and (c), respectively. The two dashed arrows mark the beginning and the end of the $(9,1)$ nanotube determined from the simultaneously detected G-band Raman signal (not shown). The blue stars denote the center-to-center distance of the nanotubes at positions along the bundle determined from (b) and (c).

Based on the image data we now estimate the efficiency and the range of energy transfer. Cross sections perpendicular to the nanotubes were taken at different locations in (Figs. 1(b),(c)) and were fit with Gaussian line shape functions to determine the in-plane position with maximum intensity for the two spectral windows (data not shown). Center-to-center distances ranging from d = 1.5 to 4 nm were found between the two nanotubes as shown in Fig. 1(d). For each distance we determined the transfer efficiency $E(d) = 1 - I(d)/I_0$ using the measured intensities $I(d)$

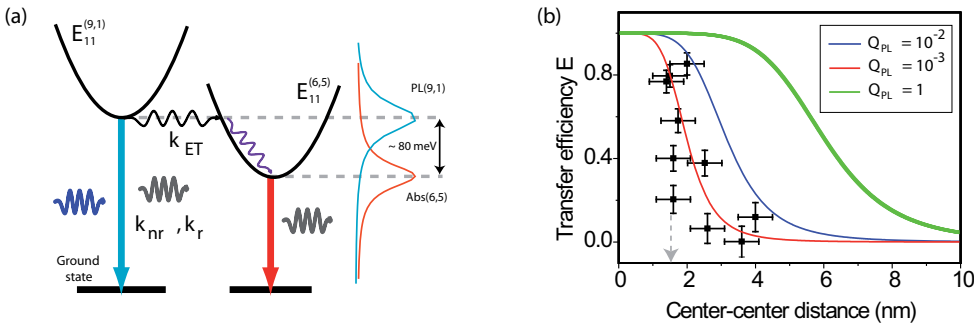

Figure 2 (a) Energy level scheme of resonant transfer in a single donor-acceptor pair formed by a $(9,1)$ and a $(6,5)$ nanotube. (b) Distance dependence of the energy transfer efficiency for a single $(9,1)$ / $(6,5)$ pair determined from the data shown in Fig. 1. The black dots with error bar represent inter-nanotube distances. The gray arrow indicates the distance at which the two nanotubes touch. The solid lines are calculated Förster energy transfer efficiencies accounting for a PL quantum yield of $Q_{PL} = 1$ (green line), $Q_{PL} = 10^{-2}$ (blue line) and $Q_{PL} = 10^{-3}$ (red line).

and I_0 of the $(9,1)$ nanotube. The data points (Fig. 2(b)) reveal a very fast decay and support our assignment of the PL intensity variations to variations of distance-dependent energy transfer.

Förster-type transfer efficiencies can be calculated for molecular systems as a function of the dipole-dipole distance. For extended quasi one dimensional nanotubes the near-field radiation pattern and thus the effective transfer rates are expected to be different [26]. Here we calculate the Förster transfer efficiency as a first estimate for the contribution of electromagnetic near-field interactions. The transfer efficiencies considering Q_{PL} formed by integrating along the z-axis of the accepting nanotube, $E(d) = 1/(1 + (Q_{PL} \int_{-\infty}^{\infty} (R_0/R)^6 dz)^{-1})$, are shown in Fig. 2(b) together with the experimentally determined values from Fig. 1. Good agreement can be seen for a quantum yield of $Q_{PL} = 10^{-3}$, a typical value discussed for nanotubes on substrates. Exciton transfer clearly depends very sensitively on the nanotube-nanotube distance and is limited to few nanometers because of competing fast non-radiative relaxation processes leading to a low Q_{PL}.

3.2 PL quenching at nanotube ends Nanotube ends are of great importance for applications as 1D wires and for understanding the effect of local defects. Theoretical modeling based on tight-binding calculations [27] and experimental results using scanning tunneling spectroscopy (STS) [28–30] indicate dramatic changes in the electronic structure towards the carbon nanotube ends. In particular, the lowest singularity in the density of states diminishes and is replaced by a single prominent peak close to the Fermi level or at higher energies depending on structural details, i.e. open or closed ends. These band modifications are confined to the nanotube end with spatial extensions of few nanometers only. Propagation of mobile excitons in the axial direction on the other hand is expected to lead to quenching at the ends resulting in reduced PL [31].

Figure 3 shows simultaneously obtained topography (a) and near-field PL (b) images of a DNA-wrapped carbon nanotube end. The nanotube topography ends at the position marked with the white dashed line, while the PL already fades out before the line. (c) plots the profiles along the black dashed lines in both (a) and (b). The line-circle curve represents the topographic height variation and the line-triangle represents the PL intensity variation. The two solid red lines are guide to the eyes. The decay of the topography profile reflects the convolution between the tip shape and the step-function representing the nanotube end. Here we interpret the position at which the topography signal dropped by a factor 2 as the end of the nanotube indicated by the blue dashed line in Fig. 3(c). The PL intensity profile clearly decays slower. The distance between the positions with signals at half maximum gives an estimated PL decay length of about 65 nm. This and other examples showing PL decay lengths in the range of 50-90 nm clearly support the idea of non-radiative decay of mobile excitons at quenching states confined to the nanotube end. Since in TENOM the optical resolution is generally found to exceed the topographic resolution [14, 13] the slower decay of the PL signal is not caused by different signal formation processes.

In summary, we investigated the exciton energy transfer between a pair of semiconducting carbon nanotubes and exciton propagation towards the nanotube ends using tip enhanced near-field microscopy. Energy transfer from a larger band gap nanotube to a smaller band gap nanotube was observed, limited to few nanometers distances because of competing fast non-radiative relaxation. Towards the end of a nanotube, PL decay is observed on a length scale of 50-90 nm and attributed to non-radiative decay at the end. Exciton mobility can also be expected to influence nanotube-nanotube coupling complicating a detailed quantification of inter-nanotube transfer phenomena.

Acknowledgements The authors wish to acknowledge Steffen Schmidt (LMU) for SEM support. This work was funded by the Deutsche Forschungsgemeinschaft (DFG-HA4405/3-1 and the Nanosystems Initiative Munich (NIM)), the U.S. Department of

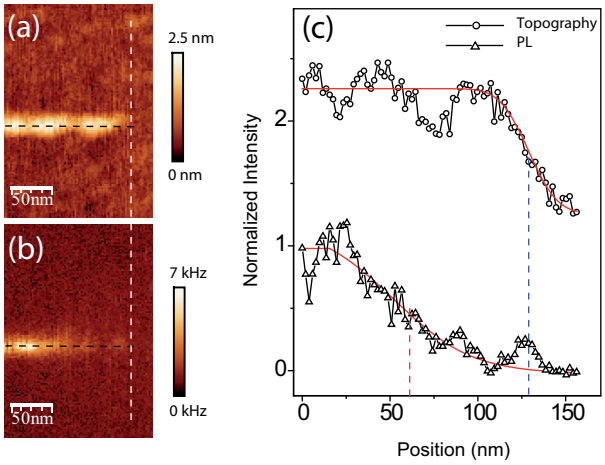

Figure 3 Simultaneously obtained topography (a) and near-field PL (b) images of a DNA-wrapped carbon nanotube end upon laser excitation at 632.8 nm. The excitation power is 5 μW. (c) shows profiles along the two black dashed lines in (a) and (b), representing topographic height and PL intensity, respectively. The blue dashed line indicates the position of the end of the nanotube taken at half of the topographic height. The PL signal exhibits slower decay. The position at which the PL signal is decreased by a factor of 2 marked by the red dashed line occurs about 65 nm before the end of the nanotube.

Energy (grant DE-FG02-05ER46207). Support from an Alfred P. Sloan Research Fellowship (M.C.H.) and a Natural Sciences and Engineering Research Council of Canada Fellowship (A.A.G.) are gratefully acknowledged. This work was also funded by the U.S. National Science Foundation under Award Numbers EEC-0647560 and DMR-0706067.

References

[1] M. J. O'Connell, S. M. Bachilo, C. B. Huffman, V. C. Moore, M. S. Strano, E. H. Haroz, K. L. Rialon, P. J. Boul, W. H. Noon, C. Kittrell, J. Ma, R. H. Hauge, R. B. Weisman, and R. Smalley, Science **297**, 593–596 (2002).
[2] E. Chang, G. Bussi, A. Ruini, and E. Molinari, Phys. Rev. Lett. **92**, 196401 (2004).
[3] C. D. Spataru, S. Ismail-Beigi, L. X. Benedict, and S. G. Louie, Phys. Rev. Lett. **92**, 077402–077405 (2004).
[4] A. Hagen, M. Steiner, M. B. Raschke, C. Lienau, T. Hertel, H. Qian, A. J. Meixner, and A. Hartschuh, Phys. Rev. Lett. **95**, 197401–197404 (2005).
[5] F. Wang, G. Dukovic, L. E. Brus, and T. F. Heinz, Phys. Rev. Lett. **92**, 177401–177404 (2004).
[6] Y. Z. Ma, J. Stenger, J. Zimmermann, S. M. Bachilo, R. E. Smalley, R. B. Weisman, and G. R. Fleming, J. Chem. Phys. **120**, 3368 (2004).
[7] H. Qian, C. Georgi, N. Anderson, A. A. Green, M. C. Hersam, L. Novotny, and A. Hartschuh, Nano Lett. **8**, 1363–1367 (2008).
[8] H. Qian, P. T. Araújo, C. Georgi, T. Gokus, N. Hartmann, A. A. Green, A. Jorio, M. C. Hersam, L. Novotny, and A. Hartschuh, Nano Lett., accepted (2008).
[9] T. Gokus, H. Harutyunyan, F. Hennrich, P. T. Araujo, M. Kappes, A. Jorio, M. Allegrini, A. A. Green, M. C. Hersam, and A. Hartschuh, Appl. Phys. Lett. **92**, 153116 (2008).
[10] L. Cognet, D. T. Tysboulski, J. D. R. Rocha, C. D. Doyle, J. M. Tour, and R. B. Weisman, Science **316**, 1465–1468 (2007).
[11] C. Georgi, N. Hartmann, T. Gokus, A. A. Green, M. C. Hersam, and A. Hartschuh, Chem. Phys. Chem., published online doi:10.1002/cphc.20080079 (2008).
[12] A. Hartschuh, H. Qian, A. J. Meixner, N. Anderson, and L. Novotny, Nano Lett. **5**, 2310–2313 (2005).
[13] Kawata, S. and Shalaev, V. M. (ed.), Tip enhancement, Advances in Nano-Optics and Nano-Photonics (Elsevier, Amsterdam, 2007).
[14] A. Hartschuh, E. J. Sánchez, X. S. Xie, and L. Novotny, Phys. Rev. Lett. **90**, 095503–095506 (2003).
[15] K. Karrai and R. D. Grober, Appl. Phys. Lett. **66**, 1842–1844 (1995).
[16] M. S. Arnold, A. A. Green, J. F. Hulvat, S. I. Stupp, and M. C. Hersam, Nature Nanotechnol. **1**, 60–65 (2006).
[17] A. A. Green and M. C. Hersam, Mater. Today **10**, 59–60 (2007).
[18] M. Zheng, A. Jagota, E. D. Semke, B. A. Diner, R. S. Mclean, S. R. Lustig, R. E. Richardson, and N. G. Tassi, Nature. Mater. **2**, 338–342 (2003).
[19] H. Jin, E. S. Jeng, D. A. Heller, P. V. Jena, R. Kirmse, J. Langowski, and M. S. Strano, Macromolecules **40**, 6731–6739 (2007).
[20] S. Reich, M. Dworzak, A. Hoffmann, C. Thomsen, and M. S. Strano, Phys. Rev. B **71**, 033402 (2004).
[21] Z. Zhu, J. Crochet, M. S. Arnold, M. C. Hersam, H. Ulbricht, D. Resasco, and T. Hertel, J. Phys. Chem. C **111**, 3831–3835 (2006).
[22] T. Hertel, R. Fasel, and G. Moos, Appl. Phys. A **75**, 449–465 (2002).
[23] P. H. Tan, A. G. Rozhin, P. Hu, V. Scardaci, W. I. Milne, and A. C. Ferrari, Phys. Rev. Lett. **99**, 137402–4 (2007).
[24] S. M. Bachilo, M. S. Strano, C. Kittrell, R. H. Hauge, R. Smalley, and R. B. Weisman, Science **298**, 2361–2366 (2002).
[25] J. A. Fagan, J. R. Simpson, B. J. Bauer, S. H. De Paoli Lacerda, M. L. Becker, J. Chun, K. B. Migler, A. R. Hight Walker, and H. E. K., J. Am. Chem. Soc. **129**, 10607–10612 (2007).
[26] I. V. Bondarev, G. Y. Slepyan, and S. A. Maksimenko, Phys. Rev. Lett. **89**, 115504–115507 (2002).
[27] A. De Vita, J. C. Charlier, X. Blase, and R. Car, Appl. Phys. A **68**, 283–286 (1999).
[28] D. L. Carroll, P. Redlich, P. M. Ajayan, J. C. Charlier, X. Blase, A. De Vita, and R. Car, Phys. Rev. Lett. **78**, 2811–2814 (1997).
[29] P. Kim, T. W. Odom, J. Huang, and C. M. Lieber, Phys. Rev. Lett. **82**, 1225–1228 (1999).
[30] L. C. Venema, J. W. Janssen, M. R. Buitelaar, J. W. G. Wildöer, S. G. Lemay, L. P. Kouwenhoven, and C. Dekker, Phys. Rev. B **62**, 5238–5244 (2000).
[31] A. Rajan, M. S. Strano, D. A. Heller, T. Hertel, and K. Schulten, J. Phys. Chem. B **112(19)**, 6211–3 (2008).